Workspace Optimization and Kinematic Performance Evaluation of 2-DOF Parallel Mechanisms

Yun-Joo Nam
Department Mechanical and Intelligent Systems Engineering, Pusan National Universiy, 30 Jangjeon-dong, Geumjeong-gu, Busan 609-735, Korea
Myeong-Kwan Park*
Research Institute of of Mechanical Technoloty, School of Mechanical Engineering, Pusan National University, 30 Jangjeon-dong, Geumjeong-gu, Busan 609-735, Korea

This paper presents the kinematics and workspace optimization of the two different 2-DOF (Degrees-of-Freedom) planar parallel mechanisms : one (called 2-RPR mechanism) with translational actuators and the other (called 2-RRR mechanism) with rotational ones. First of all, the inverse kinematics and Jacobian matrix for each mechanism are derived analytically. Then, the workspace including the output-space and the joint-space is systematically analyzed in order to determine the geometric parameters and the operating range of the actuators. Finally, the kinematic optimization of the mechanisms is performed in consideration of their dexterity and rigidity. It is expected that the optimization results can be effectively used as a basic material for the applications of the presented mechanisms to more industrial fields.

Key Words : Jacobian, Kinematics, Optimization, Parallel Mechanism, Workspace

1. Introduction

A parallel mechanism is a closed-loop chain in which a movable end-effector is connected to the fixed base by at least two serial kinematic sub-chains (Choi, 2003). This type of mechanisms can be found in several practical applications, such as pilot-training simulators, high precision-surgical tools, high speed-machine tools, and micro-positioning devices, because they have many advantages in terms of high rigidity-to-weight ratio, fast speed, high accuracy, reduced installation-space requirement, flexibility, and low inertia (Chung et al., 2003 ; Park et al., 2001 ; Wang and Liu, 2003). However, from the viewpoints of design, trajectory planning, and applications, the limited workspace and the complicated kinematic analysis resulting from the closed-loop nature of the mechanism are major disadvantages of parallel mechanisms.

To overcome these drawbacks, parallel mechanisms with the reduced number of degree-of-freedom (DOF) have attracted more and more researcher's attention in the recent robotics literatures. These reduced-DOF mechanisms can successfully perform many tasks that have to date required fully-DOF mechanisms. Moreover, they have simpler mechanical structure, simpler control system, higher speed-performance, and lower manufacturing and operating costs. Especially, they can provide a larger workspace for the remaining motion range.

Among these reduce-DOF mechanisms, 2-DOF planar parallel mechanisms are an important class in robotic mechanisms, which can follow an arbitrary curve in plane (Chung et al., 2001 ; Chung

* Corresponding Author,
E-mail : mkpark1@pusan.ac.kr
TEL : +82-51-510-2464; **FAX** : +82-51-514-0685
Research Institute of of Mechanical Technoloty, School of Mechanical Engineering, Pusan National University, 30 Jangjeon-dong, Geumjeong-gu, Busan 609-735, Korea. (Manuscript **Received** February 2, 2006; **Revised** July 8, 2006)

and Lee, 2001; Frisoli et al., 1999; Gao et al., 1998; Huang et al., 2004; Liu et al., 2003; Nam et al., 2005). Due to their usefulness in applications to high-tech machinery, such as optical device, precision-machine tool and semiconductor manufacturing machine, the study on the kinematics and design of these mechanisms with novel or old configuration is very important. Nevertheless, it is fact that most of the previous researches on the reduced-DOF mechanism have mainly concentrated on 3-DOF spatial parallel mechanisms (Birglen et al., 2002; Carretero et al., 2000; Gregorio and Parenti-Castelli, 2001; Joshi and Tsai, 2002; Kim and Tsai, 2003; Liu et al., 2001; Romdhance et al., 2002; Stock and Miller, 2003; Wolf et al., 2003).

Consequently, the goal of this paper is to perform the workspace optimization of two different conventional 2-DOF parallel mechanisms and to evaluate their kinematic performances. The presented parallel mechanisms are a kind of 5-bar link position mechanism with two actuators and three passive rotational joints. One of the mechanisms is transition-actuated, and the other is rotation-actuated. First of all, the inverse kinematics and Jacobian matrix of the presented mechanisms are derived analytically. Then, after the workspace including the input jointspace and the output workspace is symbolically analyzed, the workspace optimization of these mechanisms is performed. The results obtained in this paper can be used as a basic material in applications of these mechanisms to more various industrial fields.

2. Kinematic Analysis

As can be seen in Fig. 1, the 2-DOF parallel mechanisms presented in this paper consist of an end-effector that is connected to a fixed base by two actuated legs with kinematically identical topology. The i-th leg of the 2-RPR mechanism, by denoted l_i $(i=1,2)$, connects a passive rotational joint B_i on the base to a passive rotational joint C as the end-effector. The i-th leg of the 2-RPR mechanism is composed of the lower link l_a attached to an active rotational joint B_i on the base and the upper link l_b connected to the lower one

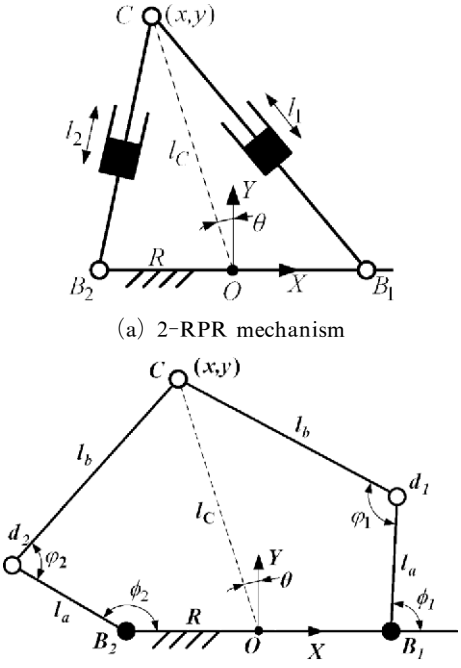

(a) 2-RPR mechanism

(b) 2-RRR mechanism

Fig. 1 Kinematic configuration of the 2-DOF parallel mechanisms

via a rotational passive joint d_i. Here, the rotation angle of the actuator is denoted by ϕ_i. In this paper, the symbol 'R' and 'P' designate a rotational joint and a transitional one, respectively.

For the purpose of kinematic analysis, a fixed reference coordinate frame O_XY is attached to the base at point O. Let us denote the position of the end-effector with respect to the base as the coordinate (x,y). The distance between O and C, $L_C=\sqrt{x^2+y^2}$, and the rotation angle $\theta=\arctan(-x/y)$ are additionally introduced.

2.1 Inverse kinematics

The inverse kinematics is to find a set of input joint variables for a given position of the end-effector with respect to the base. For the presented mechanisms, the output variables (x,y) are given, and the input joint variables (l_1, l_2) or (ϕ_1, ϕ_2) are to be found.

2.1.1 2-RPR mechanism

Referring to Fig. 1, the closed-loop equation of the 2-RPR mechanism can be obtained as

$$\begin{cases}(x-R)^2+y^2=l_1^2\\(x+R)^2+y^2=l_2^2\end{cases} \quad (1)$$

From the above equation, the inverse kinematic solution of the presented mechanism is given in the closed-form as follows

$$\begin{cases}l_1=\pm\sqrt{(x-R)^2+y^2}\\l_2=\pm\sqrt{(x+R)^2+y^2}\end{cases} \quad (2)$$

There are four possible solutions for the inverse kinematics problem. However, since only positive leg lengths should be taken into consideration for real applications, a unique solution to the inverse kinematics can be found by taking the sign '+' from '±' in Eq. (2).

2.1.2 2-RRR mechanism

The closed-loop equation of the 2-RRR mechanism can be described from Fig. 1(b) as

$$\begin{cases}(x-R-l_a\cos\phi_1)^2+(y-l_a\sin\phi_1)^2=l_b^2\\(x+R-l_a\cos\phi_2)^2+(y-l_a\sin\phi_2)^2=l_b^2\end{cases} \quad (3)$$

Substituting the following trigonometric identities in Eq. (3) and rearranging,

$$\cos\phi_i=\frac{1-t_i^2}{1+t_i^2},\ \sin\phi_i=\frac{2t_i}{1+t_i^2},\ t_i=\tan(\phi_i/2) \quad \text{for } i=1,2 \quad (4)$$

we can obtain square polynomials in t_i as follows

$$(\gamma_i-\alpha_i)t_i^2+2\beta_i t_i+(\gamma_i+\alpha_i=0)$$

where

$$\alpha_1=2l_a(x-R),\ \beta_1=2l_a y,\ \gamma_1=-(\alpha_1^2+\beta_1^2)/(4l_a^2)+l_b^2-l_a^2$$

$$\alpha_2=2l_a(x+R),\ \beta_2=2l_a y,\ \gamma_2=-(\alpha_2^2+\beta_2^2)/(4l_a^2)+l_b^2-l_a^2$$

Hence, the closed solution to the inverse kinematic for the presented mechanism can be obtained as

$$\phi_i=\begin{cases}2\arctan\left(\dfrac{-\beta_i+\sqrt{\alpha_i^2+\beta_i^2-\gamma_i^2}}{r_i-\alpha_i}\right) & \text{for } (\gamma_i-\alpha_i)\neq 0\\ -(r_i+\alpha_i)/(2\beta_i) & \text{for } (\gamma_i-\alpha_i)=0\end{cases} \quad (6)$$

from which we can see that the mechanism has four possible solutions to the inverse kinematics. The kinematic configuration in Fig. 1(b) is obtained by taking the sign '+' for $i=1$ and '−' for $i=2$ from '±' in Eq. (6). This selection is preferred in order to exclude the mechanical interference between the actuated legs, which may occur in other three configurations.

2.2 Jacobain matrix

For the given mechanisms, the input-output velocity transmission relationship between the end-effector and the actuators can be derived by differentiating the kinematic closure equations with respect to time as follows

$$\mathbf{J}_q\dot{\mathbf{q}}=\mathbf{J}_x\dot{\mathbf{x}} \quad (7)$$

where $\dot{\mathbf{q}}\in\{[\dot{l}_1,\dot{l}_2]^T,\ [\dot{\phi}_1,\dot{\phi}_2]^T\}$ is the input velocity of the actuators, $\dot{\mathbf{x}}=[\dot{x},\dot{y}]^T$ is the output velocity of the end-effector, $\mathbf{J}_q=\Re^2$ is the inverse Jacobian matrix, and $\mathbf{J}_x=\Re^2$ is the forward Jacobian matrix. Therefore, the Jacobian matrix of the presented parallel mechanisms can be defined as

$$\mathbf{J}=\mathbf{J}_x^{-1}\mathbf{J}_q \quad (8)$$

2.2.1 2-RRR mechanism

Differentiating Eq. (1) with respect to time yields

$$\begin{cases}(x-R)\dot{x}+y\dot{y}=l_1\dot{l}_1\\(x+R)\dot{x}+y\dot{y}=l_2\dot{l}_2\end{cases} \quad (9)$$

from which the inverse and forward Jacobian matrices are, respectively, obtained as

$$\mathbf{J}_q=diag(l_1,l_2) \quad (10)$$

$$\mathbf{J}_x=\begin{bmatrix}x-R & y\\ x+R & y\end{bmatrix} \quad (11)$$

Since the singularities of a mechanism can be generally examined where $\mathbf{J}_q$, $\mathbf{J}_x$, or both become singular, the singularities of the 2-RPR mechanism are found from

$$\det[\mathbf{J}]=\det[\mathbf{J}_q]\cdot\det[\mathbf{J}_x]=-2Ryl_1l_2 \quad (12)$$

Therefore, the singularities of the mechanism exists on the x axis ($y=0$), since only positive leg lengths ($l_i>0$) and geometric parameter ($R>0$) should be taken such that the mechanism can be effectively perform the required tasks.

2.2.2 2-RRR mechanism

Differentiating Eq. (3) with respect to time yields

$$X_i\dot{x}+Y_i\dot{y}=-l_a(X_i\sin\phi_i-Y_i\sin\phi_i)\dot{\phi}_i \quad \text{for } i=1,2 \quad (13)$$

where

$$X_1=x-R-l_a\cos\phi_1,\ Y_1=y-l_a\sin\phi_1$$

$$X_2=x+R-l_a\cos\phi_2,\ Y_2=y-l_a\sin\phi_2$$

From Eq. (13), the inverse and forward Jacobian matrices of the given mechanism are, respectively, given by

$$\mathbf{J}_q=diag\left(-l_a(X_1\sin\phi_1-Y_1\cos\phi_1),\ -l_a(X_2\sin\phi_2-Y_2\cos\phi_2)\right) \tag{14}$$

$$\mathbf{J}_x=\begin{bmatrix}X_1 & Y_1\\ X_2 & Y_2\end{bmatrix} \tag{15}$$

Then, the singularities of the 2-RRR mechanism can be analytically found from the following relations

$$X_1Y_2-X_2Y_1=0 \text{ or } X_i\sin\phi_i-Y_i\cos\phi_i=0 \tag{16}$$

of which, the former corresponds to the kinematic configuration where the upper link of at least one actuated leg is positioned parallel to its lower link, and the latter where two upper links get parallel to each other. Therefore, these conditions should be adequately removed at the design stage of the mechanism so that the singularities dose not exist within the workspace of the mechanism,

3. Workspace Analysis

The workspace of a mechanism is one of important factors dominating its kinematic performance. Especially, since parallel mechanisms suffer from smaller workspace, compared to serial ones, it is very important to analyze the size and the shape of their workspace in the viewpoint of industrial applications.

The workspace of the presented mechanisms is defined as a set of all the output variables (x,y) at which the end-effector C can reach. It depends on the kinematic constraints including the mechanism architecture, the mobility of each actuated leg, and the link interferences (Gregorio, 2002). In this study, in order to disregard the mechanical interferences between the links and joints, the rotation angle of the end-effector is restricted to $\theta\in[-\pi/2,\pi/2]$. In addition, the operating range of the transitional actuators for the 2-RPR mechanism is limited to $l_1, l_2\in[l_{\min}, l_{\max}]$, where $l_{\min}$ and $l_{\max}$ denote the minimum and maximum lengths, respectively. And, the allowable rotation angle of the passive rotational joints for the 2-RRR mechanism is constrained to $\varphi_1\equiv\angle B_id_iC\in[0.\pi]$ in order to avoid singular conditions.

3.1 Output workspace

The outer boundary of the output workspace is determined where at least one actuated leg is perfectly stretched ($l_i=l_{\max}$ or $\varphi_i=\pi$), and the inner boundary where, for the 2-RPR mechanism, at least one actuated leg has its minimal length ($l_i=l_{\min}$) and for the 2-RRR mechanism, at least one passive joint reaches at zero rotation angle ($\varphi_i=0$). Then, for the rotational angle of the end-effector, θ, the maximally and minimally reachable distances from O to C can be, respectively, derived from the kinematic constraining relations (1) and (3), as follows

$$\begin{cases}l_{CM}(\theta)=-R\,\mathrm{sgn}(\theta)\sin\theta+\sqrt{\tilde{l}^2-R^2\cos^2\theta}\\ l_{Cm}(\theta)=-R\,\mathrm{sgn}(\theta)\sin\theta+\sqrt{\hat{l}^2-R^2\cos^2\theta}\end{cases} \tag{17}$$

where

$$\tilde{l}=\begin{cases}l_{\max} & \text{for } 2-RPR\\ l_a+l_b & \text{for } 2-RRR\end{cases},\quad \hat{l}=\begin{cases}l_{\min} & \text{for } 2-RPR\\ l_b-l_a & \text{for } 2-RRR\end{cases}$$

and $\mathrm{sgn}(\theta)$ is the signum function. It is noted that for any $\theta\in[-\pi/2,\pi/2]$, the necessary condition in order that there exist l_{CM} and l_{Cm} in Eq. (17) as the real values is equal to $\{\tilde{l},\hat{l}\}\geq R$.

3.2 Input jointspace

The input jointspace of a mechanism is defined as a set of all the joint variables at which the output variables (x,y) as the real values can be obtained from the kinematic constraining relation.

For the 2-RPR mechanism, the output of the end-effector can be obtained from Eq. (1) as follows

$$\begin{cases}x=(l_2^2-l_1^2)/(4R)\\ y=\sqrt{l_1^2-(x-R)^2}=\sqrt{l_2^2-(x+R)^2}\end{cases} \tag{18}$$

from which we can see that the sufficient-necessary condition in order that there exists y in real domain is to be

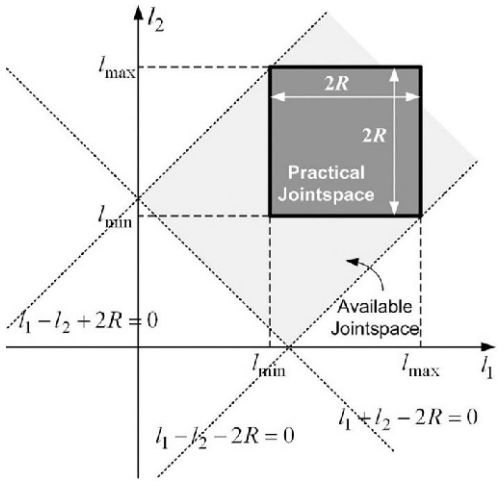

(a) Practical joint-space for 2-RPR mechanism

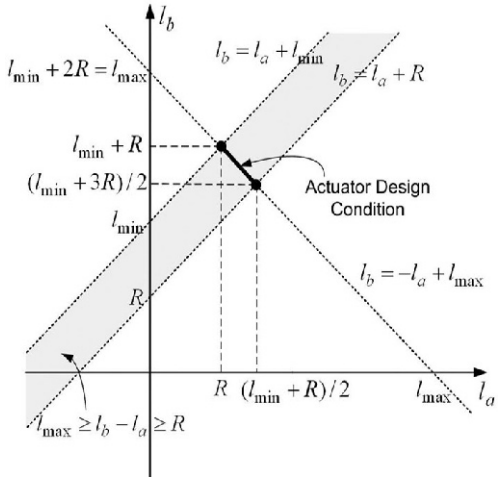

(b) Constraints of the design parameters for 2-RRR mechanism

Fig. 2 Jointspace and geometric constraints for the real outputs of the mechanisms

$$l_1^2 - (x-R)^2 \geq 0,\ l_2^2 - (x+R)^2 \geq 0$$
$$\Leftrightarrow (l_1 - l_2 + 2R)(l_1 + l_2 - 2R)(l_1 - l_2 - 2R) \leq 0 \quad (18)$$

Considering both two actuated legs has the kinematically identical topology and the mechanism should have the output workspace as large as possible, the operating range of two actuators is constrained as can be seen in Fig. 2(a).

$$R \leq l_{min} \leq l_i \leq l_{max} = l_{min} + 2R \quad (20)$$

where it is noted that the minimal length of the actuated leg l_{min} is a major design parameter used at next 'Workspace Optimization' section.

For the 2-RRR mechanism, it is difficult to analytically derive the constraining relation for the input variables (ϕ_1, ϕ_2), since they are given as the function of the output (x, y) and the length of the lower and upper links. Also, the rotational actuator does not provide any constraint to the output workspace of the presented mechanism due to its nature in wide operating range. On the other hand, the rotation angle φ_i of the passive rotational joint d_i is restricted to $[0, \pi]$ in order to avoid the singular configurations of the mechanism, and it can be expressed by

$$\varphi_i = \arccos\left(\frac{l_a^2 + l_b^2 - l_i^2}{2 l_a l_b}\right) \quad (21)$$

Then, matching the limit values of the above equation to Eq. (20), that is, $\varphi_i = 0$ to l_{max} and $\varphi_i = \pi$ to l_{min}, and rearranging yield the following constraints for the lower and upper links of the mechanism, as can be seen in Fig. 2(b).

$$\begin{cases} l_{max} = l_a + l_b \\ R \leq l_b - l_a \leq l_{min} \end{cases} \Leftrightarrow \begin{cases} R \leq l_a \leq (l_{min} + R)/2 \\ (l_{min} + 3R)/2 \leq l_b \leq l_{min} + R \end{cases} \quad (22)$$

Here, it is noted that Eq. (22) is used as the constraining condition for the design parameters at next 'Workspace optimization' section.

4. Workspace Optimization

In general, parallel mechanisms have smaller workspace than serial counterparts. Hence, the workspace size of such a mechanism should be maximized. However, a try to design the mechanism in perspective of its maximal workspace may lead to undesirable kinematic characteristics such as poor dexterity and/or rigidity. Therefore, the qualitative evaluation of workspace should be performed during optimizing it.

4.1 Performance indices

4.1.1 Global conditioning index (GCI)

The first performance index used in this paper as an objective function to be maximized is the global conditioning index (Chung et al., 2003; Huang et al., 2004; Kim and Tsai, 2003), which is defined as

$$\eta_1=\frac{\int_W 1/\kappa\, dW}{\int_W dW} \tag{23}$$

where dW is differential workspace of the mechanism, and κ is the condition number of the Jacobian $\mathbf{J}$ in Eq. (8) at a given position of the end-effector within the workspace. The workspace W can be obtained by using (17) as

$$W=\int_W dW=\frac{1}{2}\int_{\pi/2-\varepsilon}^{\pi/2+\varepsilon}(l_{CM}^2-l_{Cm}^2)\,d\theta \tag{24}$$

where $\varepsilon>0$ is an infinitesimal angle introduced to avoid the singular conditions. This performance index measuring the mean value of the isotropy index $1/\kappa$ over the workspace size W is used to evaluate how uniformly the end-effector can move in arbitrary direction within the workspace. This index gives a measure of kinematic performance independent of the workspace sizes varying according to design candidates, since it is normalized by the workspace size.

4.1.2 Global resistivity index (GRI)

When a mechanism performs a given task, the end-effector exerts force onto its environment. The reaction force will cause the end-effector to be deflected away from its desired location. Intuitively, the amount of deflection is a function of the applied force and the rigidity of the mechanism. Thus, the rigidity of a mechanism has a direct impact on its position accuracy. The second performance index (Choi, 2003; Joshi and Tsai, 2002) introduced for measuring the ability of the mechanism to resist the externally applied forces is defined by

$$\eta_2=\frac{\int_W \bar{\omega}\, dW}{\int_W dW} \tag{25}$$

where $\bar{\omega}=1/|\det(\mathbf{J})|=|\det(\mathbf{J}^{-1})|$ is the inverse of the manipulability. Similarly to the isotropy index, this index is normalized by the workspace size, and therefore, is independent of the differing workspace size of design candidates.

4.1.3 Space utilization index (SUI)

Since the first two performance indices are normalized by the workspace size, they have the limitation to consider the workspace size of a mechanism. Hence, the workspace size of the mechanism is evaluated by the space utilization index (Stock and Miller, 2003) expressed as

$$\eta_3=\frac{\int_W dW}{S} \tag{26}$$

where S represents the size of the smallest rectangle enclosing the workspace size. This performance index reflects the ratio of the workspace size to the physical space size required for all possible motions of the end-effector. This index bounded by the range of $[0,1]$ is dimensionless, and therefore, its value is independent of the overall scale of each design candidates to which it is applied.

The workspace optimization of the mechanisms studied in this paper requires a practical performance index comprising multiple indices mentioned above. The values of the three performance indices may be distributed in different ranges. Hence, in order to make a meaningful comparison among them and to prevent simply cancellations between denominators and numerators during the combination process, each of the three indices is normalized by using its maximum and minimum values. Then, the composite performance index (CPI) for the workspace optimization of the presented mechanisms can be defined as

$$\eta=w_1\hat{\eta}_1+w_2\hat{\eta}_2+w_3\hat{\eta}_3 \tag{27}$$

where

$$\hat{\eta}_i=\frac{\eta_i-\min(\eta_i)}{\max(\eta_i)-\min(\eta_i)}$$

and $w_i(i=1\sim3)$ is positive weighting factor specifying relative importance placed on each performance index by the designer.

4.2 Numerical optimizations

The objective of the workspace optimization is to determine a set of the design parameters of the mechanism leading to the composite performance index to be maximized. The design parameters of the 2-RPR mechanism include the minimal length of the transitional actuator, $l_{\min}$ in Eq. (20), and the size of the base R. On the other hand, the

design parameters of the 2-RRR mechanism are the lengths of the lower and upper links, l_a and l_b in Eq. (22), and the size of the base R. Therefore, if all design parameters are non-dimensioned with respect to R such that the obtained results are applicable to any scale of the mechanisms, the workspace optimization problem for the presented mechanisms can be redefined as follows

$$\underset{R=1,l_{\min},l_a}{Maximize}\ (\eta)\ \text{subject to}\ \begin{cases}\text{Eq. (20) for 2-}RPR\text{ mech}\\ \text{Eq. (22) for 2-}RRR\text{ mech}\end{cases} \quad (28)$$

A numerical computation is carried out in the MATLAB environment. The numerical integrals for Eqs. (23) and (24) are approximated by the following discrete sum :

$$\frac{\int_W I\,dW}{\int_W dW}=\frac{1/2\sum_{m=1}^{M}\sum_{n=1}^{N}[I_{mn}(l_{c,m+1}{}^2-l_{c,m}^2)\Delta\theta_n]}{1/2\sum_{m=1}^{M}\sum_{n=1}^{N}[(l_{c,m+1}^2-l_{c,m}^2)\Delta\theta_n]} \quad (29)$$

where $l_{c,j}$ is the distance from the origin O to j-th node of M equally meshed $l_c\in[l_{cm}, l_{cM}]$, and $\Delta\theta_j$ is the j-th differential angle of N equally meshed $\theta\in[-\pi/2+\varepsilon, \pi/2-\varepsilon]$. $I_{mn}\in\{1/\kappa, \bar{\omega}\}$ represents the value of the index at node (m, n) generated by forming a uniformly distributed grid between the inner and outer boundaries of the workspace. The workspace is split into $M\times N$ sectors, and its area is calculated by their sum. Using $(M,N)=(200,300)$, the computational errors of the workspace size in several situations are estimated to be less than 3%.

The performance indices and the corresponding design parameters of the 2-RPR and 2-RRR mechanisms obtained with respect to the selected set of the weighting factors are represented in Tables 1 and 2, respectively. For the 2-RPR mechanism, the variation of each performance index according to the weighting factor set remains within 0.62% on the basis of the maximum value,

Table 1 Numerical examples of the workspace optimization for the 2-RPR mechanism

(w_1, w_2, w_3)	$\frac{l_{\min}}{R}$	$\frac{l_{\max}}{R}$	GCI	GRI	SUI	CPI
			Max : 0.55592	Max : 0.80577	Max : 0.45157	Max : 2.99388
			Min : 0.22991	Min : 0.437	Min : 0.23765	Min : 0.0
(1, 0, 0)	1.01	3.01	0.55592	0.80577	0.44876	2.98687
(0, 1, 0)	1.01	3.01	0.55592	0.80577	0.44876	2.98687
(0, 0, 1)	1.0	3.0	0.55527	0.80423	0.45157	2.99388
(1, 1, 0)	1.01	3.01	0.55592	0.80577	0.44876	2.98687
(0, 1, 1)	1.0	3.0	0.55527	0.80423	0.45157	2.99388
(1, 0, 1)	1.0	3.0	0.55527	0.80423	0.45157	2.99388
(1, 1, 1)	1.0	3.0	0.55527	0.80423	0.45157	2.99388

Table 2 Numerical examples of the workspace optimization for the 2-RRR mechanism

(w_1, w_2, w_3)	$\frac{l_{\min}}{R}$	$\frac{l_a}{R}$	$\frac{l_b}{R}$	GCI	GRI	SUI	CPI
				Max : 0.7078	Max : 2.42518	Max : 0.45216	Max : 2.58808
				Min : 0.25832	Min : 0.19528	Min : 0.1607	Min : 0.33213
(1, 0, 0)	2.08	1.39	2.69	0.7078	0.78609	0.29929	1.72942
(0, 1, 0)	1.12	1.0	2.12	0.5669	2.42518	0.42356	2.58634
(0, 0, 1)	1.0	1.0	1.0	0.50139	2.38451	0.45216	2.52255
(1, 1, 0)	1.36	1.0	2.36	0.62059	2.36238	0.38094	2.52834
(0, 1, 1)	1.3	1.06	2.24	0.63349	1.63565	0.39044	2.26439
(1, 0, 1)	1	1.0	1.0	0.50139	2.38451	0.45216	2.52255
(1, 1, 1)	1.15	1.0	2.15	0.57756	2.424	0.41744	2.58808

which is insignificant. On the other hand, for 2-RRR mechanism, the variation with respect to the weighting factor set is maximally given by 29.16% in GCI, 67.59% in GRI, and 33.81% in SUI. From these results, we can see that compared to the 2-RPR mechanism, the 2-RRR mechanism has more flexibility in the selection of the weighting factor set for the composite performance index. In other words, the design parameters of the 2-RRR mechanism should be reasonably determined in consideration of its application area. Moreover, it can be seen that in the case of in-

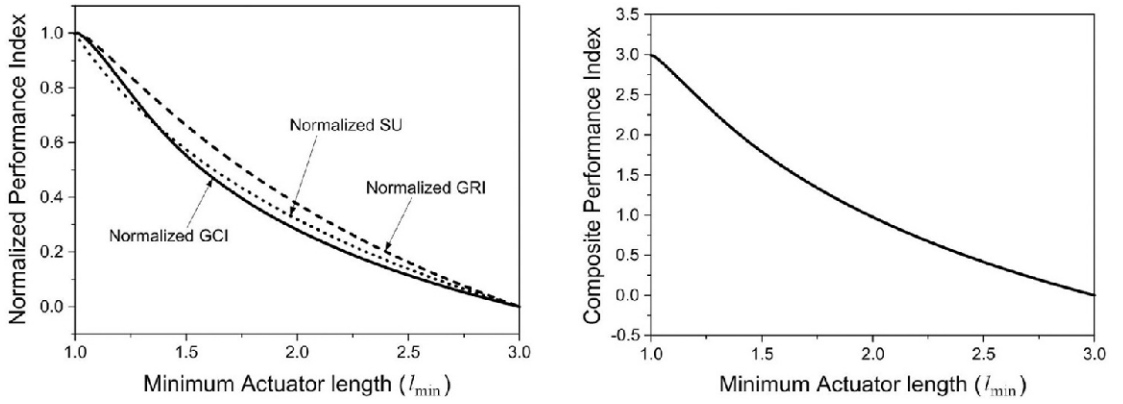

(a) 2-RPR mechanism

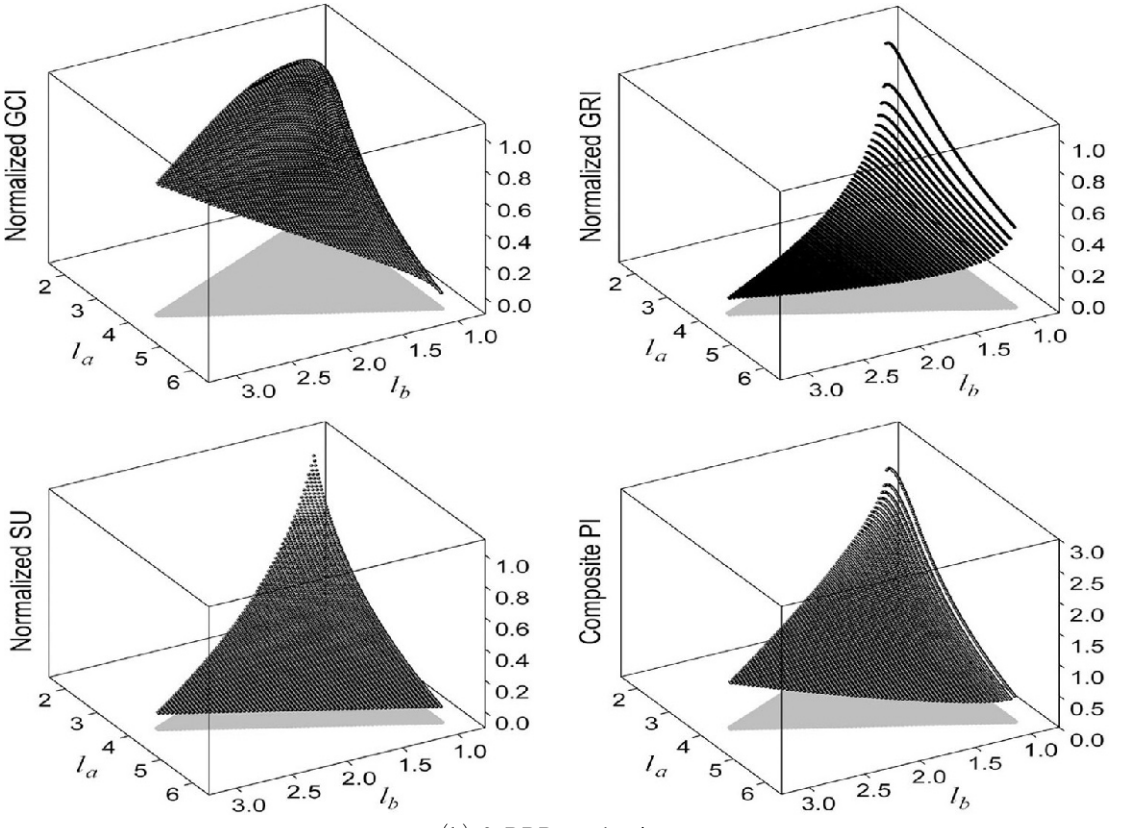

(b) 2-RRR mechanism

Fig. 3 Composite performance indices

cluding all the performance indices in Eqs. (23), (25) and (26), the maximum CPI is obtained and the each performance index is close to its maximum value. This clearly shows that the CPI given in Eq. (27) is reasonable for the workspace optimization of the presented 2-DOF parallel mechanisms. Therefore, in this paper, the optimal design parameter sets for the 2-RPR and 2-RRR mechanisms are, respectively, chosen as $(l_{\min}/R, l_{\max}/R)=(1.0, 3.0)$ and $(l_a/R, l_b/R)=(1.0, 2.15)$ for the purpose of the comparison study on their kinematic performances. Fig. 3 shows the CPI obtained at $(w_1, w_2, w_3)=(1, 1, 1)$, with respect to the design parameters.

Figure 4 shows the local conditioning index and the local resistivity index for the optimized 2-RPR mechanism. As can be seen from the conditioning index of Fig. 4(a), the singularities of the mechanism exist near the x axis ($y=0$), which corresponds to the result in Eq. (12). Since these singularities are placed on the pointed ends of the workspace, they can be effectively excluded at the path planning stage such that the mechanism feels free from the singularity problem. As can be seen in Fig. 4(b), the resistivity index is shapely decreased at which the mechanism lies on the singular configuration, from which we can indirectly see that the manipulability of the mechanism is significantly increased in a specific direction, considering $\bar{\omega}$ of Eq. (25). On the other hand, it can be clearly seen that the contour of the conditioning index is distributed within the workspace similarly to that of the resistivity index. This corresponds to the fact that the different selection of the weighting factor has little effect on the kinematic performance of the mechanism, as previously shown in Table 1.

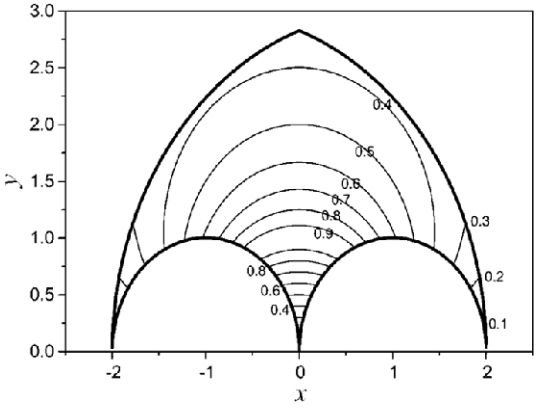

(a) Conditioning index : dexterity

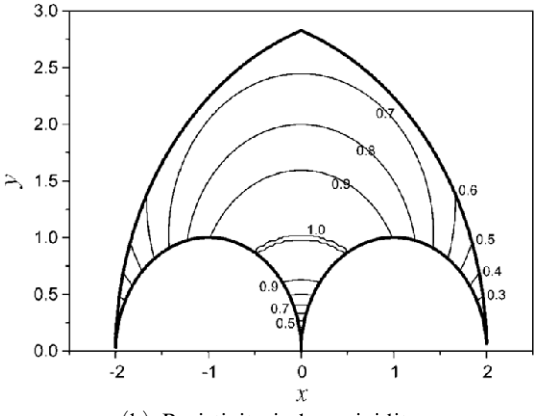

(b) Resistivity index : rigidity

Fig. 4 Local performance indices of 2-RPR mechanism

Figure 5 shows the local conditioning index and the local resistivity index for the optimized 2-RRR mechanism. Similarly to the 2-RPR mechanism, it is verified from the conditioning index in Fig. 5(a) that the singular configuration of the 2-RRR mechanism is obtained when the end-effector reaches at x axis. Especially, considering that the contour of the conditioning index is distributed similarly to the boundaries of the workspace, it can be seen that this mechanism provides more stable dexterity than the 2-RPR one. As shown in Fig. 5(b), the resistivity index is significantly increased when the end-effector is positioned close to the boundaries of the workspace. This means that the manipulability of two rotational actuators is rapidly decreased at the boundaries of the workspace. Moreover, it can be clearly seen that 2-RRR mechanism displays superior rigidity property to the 2-RPR counterpart. From these facts, it can be concluded that the 2-RRR mechanism is more effective in perspective of the rigidity than dexterity. This can be also verified from the fact that the result optimized by using only GRI is almost identical to the result obtained by using all performance indices, as indicated in Table 2.

Figure 6 shows the kinematic configurations of the optimized mechanisms, which are obtained

when the end-effector moves along the boundaries of the workspace. For the 2-RPR mechanism, all boundaries of the workspace are generated by the operating limits of the actuators, and the singular configurations occur only on the x axis. On the other hand, the singular configurations of the 2-RRR mechanism are obtained on the x axis as well as the boundaries of the workspace. Therefore, the user of the 2-RRR mechanism should take care that the end-effector does not reach on these singularities.

In addition, the trajectories of the actuators

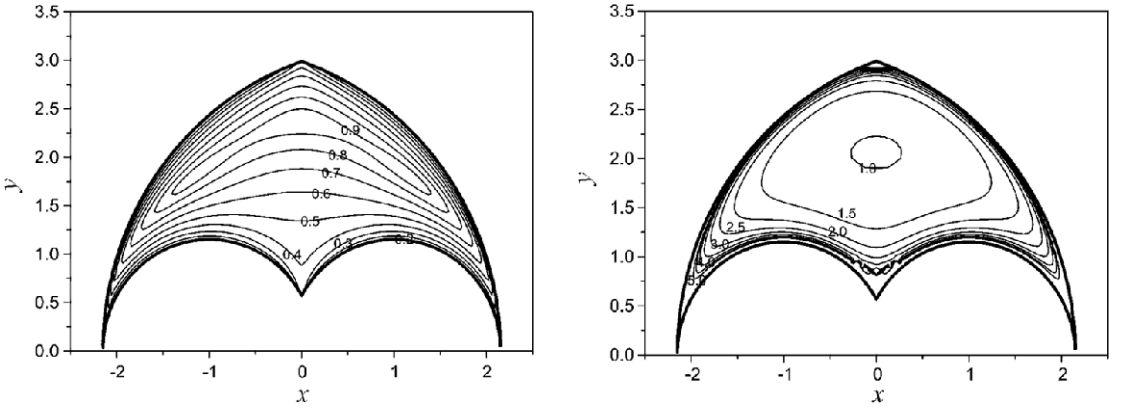

(a) Conditioning index : dexterity (b) Resistivity index : rigidity

Fig. 5 Local performance indices of 2-RRR mechanism

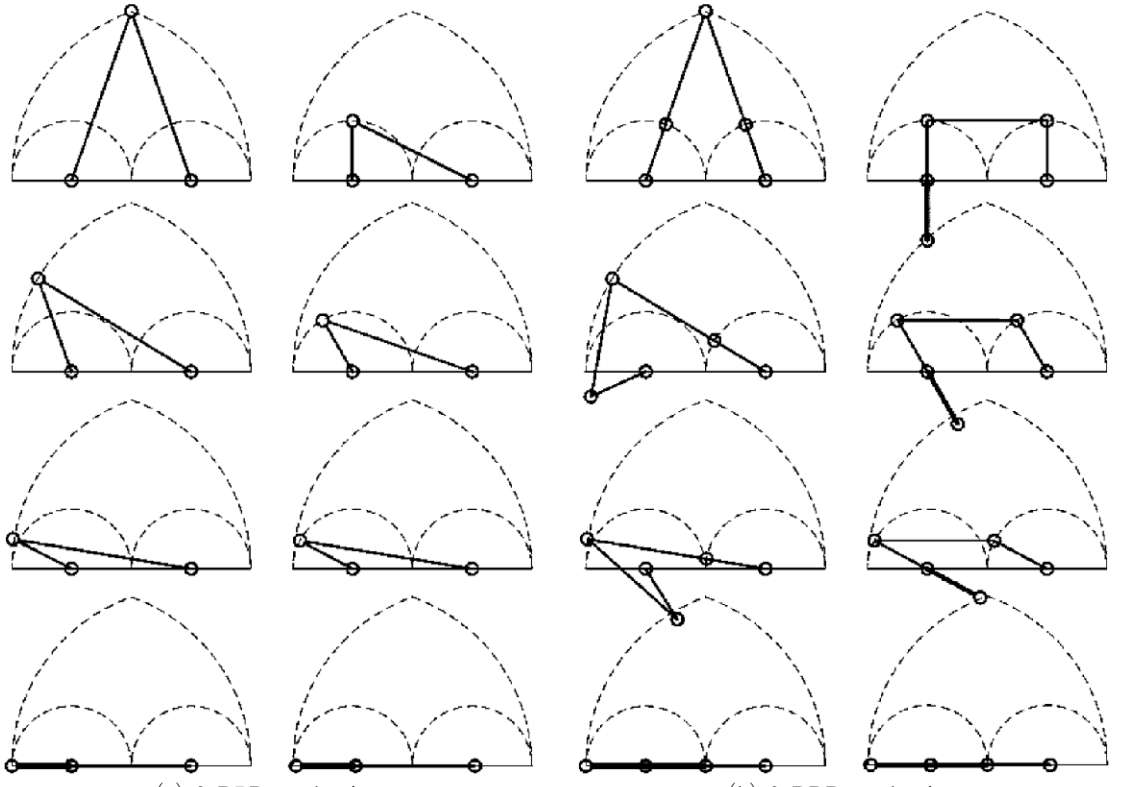

(a) 2-RPR mechanism (b) 2-RRR mechanism

Fig. 6 Workspace and panoramic motions of the optimized mechanisms

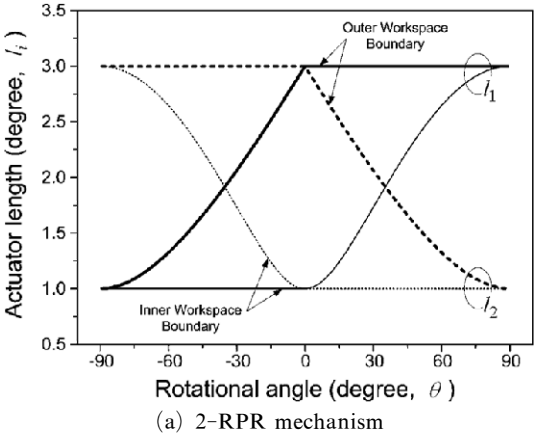

(a) 2-RPR mechanism

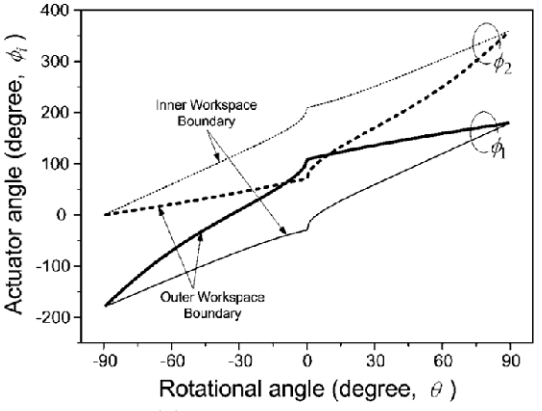

(b) 2-RRR mechanism

Fig. 7 Operating range of the actuators for the optimized mechanisms according to the rotation angle of the end-effector

obtained while the end-effector moves along the boundaries of the workspace are depicted in Fig. 7. From Fig. 7(a), it can be verified that the transitional actuators of the 2-RPR mechanism are operated within their operating limits presented in Eq. (20). On the other hand, The results in Fig. 7(b) can be used as a useful material for avoiding the singularity loci at the joint trajectory planning stage.

5. Conclusions

In this paper, the kinematic analysis and the workspace optimization of two different 2-DOF planar parallel mechanisms were performed, of which one with the translational actuators and the other with the rotational actuators.

First of all, the kinematic analysis for the mechanisms is performed : the inverse kinematics problem was solved in closed form, and the Jacobian matrix was analytically derived from the kinematic constraining relations. Then, the workspace of the mechanisms was analyzed on the basis of the output workspace of the end-effector and the input jointspace of the actuators. The operating range and the constraining conditions for the design parameter, which were obtained from the input jointspace analysis, could be very effectively used at the workspace optimization stage. Finally, the workspace optimization of the mechanisms was performed by using the composite performance index introduced in the perspective of the dexterity, rigidity, and space utilization. Therefore, it is expected that the results in this paper can be effectively used as a basic design material in application of the presented mechanisms to various industrial areas.

References

Birglen, L., Gosselin, C., Pouliot, N., Monsarrat, B. and Laliberté, T., 2002, "SHaDe, A New 3-DOF Haptic Device," *IEEE Trans. on Robotics and Automation*, Vol. 18, No. 2, pp. 166～175.

Carretero, J. A., Podhorodeski, R. P., Nahon, M. A. and Gosselin, C. M., 2000, "Kinematic Analysis and Optimization of a New Three Degree-of-Freedom Spatial Parallel Manipulator," *ASME J. of Mechanical Design*, Vol. 122, pp. 17～24.

Choi, K. B., 2003, "Kinematic Analysis and Optimal Design of 3-PPR Planar Parallel Manipulator," *KSME International Journal*, Vol. 17, No. 4, pp.528～537.

Chung, J. -H., Ko, S. -Y., Kwon, D. -S., Lee, J.,-J., Yoon, Y. -S. and Won, C. -H., 2003, "Robot-Assisted Femoral Stem Implantation Using an Intramedulla Gauge," *IEEE Trans. on Robotics and Automation*, Vol. 19, No. 5, pp. 855～892.

Chung, Y. -H. and Lee, J. -W., 2001, "Design of a New 2 DOF Parallel Mechanism," *Proc. of IEEE/ASME Int. Conf. on Advanced Intelligent Mechatronics*, Como, Italy, pp. 129～134.

Chung, Y.-H., Lee, J.-W., Sung, Y.-G. and Joo, H.-H., 2001, "Dynamics and Control of 2-DOF 5-Bar Parallel Manipulator with Closed Chain," *International Journal of the Korean Society of Precision Engineering*, Vol. 2, No. 1, pp. 5~10.

Frisoli, A., Prisco, G. M., Salsedo, F. and Bergamasco, M., 1999, "A Two Degrees-of-Freedom Planar Haptic Interface with High Kinematic Isotropy," *Proc. of IEEE Int. Workshop on Robot and Human Interaction*, Pisa, Italy, pp. 297~302.

Gao, F., Liu, X. and Gruver, W. A., 1998, "Performance Evaluation of Two-Degree-of-Freedom Planar Parallel Robots," *Mechanism and Machine Theory*, Vol. 33, No. 6, pp. 661~668.

Gregorio, R. D. and Parenti-Castelli, V., 2001, "Position Analysis in Analytical Form of the 3-PSP Mechanism," *ASME J. of Mechanical Design*, Vol. 123, pp. 51~57.

Gregorio, R. D., 2002, "Analytic Determination of Workspace and Singularities in a Parallel Pointing System," *J. of Robotic Systems*, Vol. 19, pp. 37~43.

Huang, T., Li, M., Li, Z., Chetwynd, D. G. and Whitehouse, D. J., 2004, "Optimal kinematic Design of 2-DOF Parallel Manipulators With Well-Shaped Workspace Bounded by a Specified Conditioning Index," *IEEE Trans. on Robotics and Automation*, Vol. 20, No. 3, pp. 538~543.

Joshi, S. and Tsai, L.-W., 2002, "A Comparison Study of Two 3-DOF Parallel Manipulators: One with Three and the Other with Four Supporting Legs," *Proc. IEEE Int. Conf. on Robotics and Automation*, DC, pp. 3690~3697.

Kim, H. S. and Tsai, L.-W., 2003, "Kinematic Synthesis of a Spatial 3-RPS Parallel Manipulator," *ASME J. of Mechanical Design*, Vol. 125, pp. 92~97.

Liu, X.-J., Tang, X. and Wang, J., 2003, "A Novel 2-DOF Parallel Mechanism Based Design of a New 5-Axis Hybrid Machine Tool," *Proc. of IEEE Int. Conf. on Robotics and Automation*, Taipei, Taiwan, pp. 3990~3995.

Liu, X.-J., Wang, J., Gao, F. and Wang, L.-P., 2001, "On the Analysis of a New Spatial Three-Degree-of-Freedom Parallel Manipulator," *IEEE Trans. on Robotics and Automation*, Vol. 17, No. 6, pp. 959~968.

Nam, Y.-J., Lee, Y.-H. and Park, M. K., 2005, "Kinematic Analysis and Optimal Design of 2RPR-RP Parallel Manipulator," *Tran. of the Korean Society of Mechanical Engineering* (*Part A*), Vol. 29, No. 11, pp. 1509~1517.

Park, M. K., Lee, M. C., Yoo, K. S., Son, K., Yoo, W. S. and Han, M. C., 2001, "Development of the PNU Vehicle Driving Simulator and Its Performance Evaluation," *Proc. of IEEE Int. Conf. on Robotics and Automation*, Seoul, Korea, pp. 2325~2330.

Romdhane, L., Affi, Z. and Fayet, M., 2002, "Design and Singularity Analysis of a 3-Translational-DOF In-Parallel Manipulator," *ASME J. of Mechanical Design*, Vol. 124, pp. 419~426.

Stock, M. and Miller, K., 2003, "Optimal Kinematic Design of Spatial Parallel Manipulators: Application to Linear Delta Robot," *ASME J. of Mechanical Design*, Vol. 125, pp. 292~301.

Wang, J. and Liu, X.-J., 2003, "Analysis of a Novel Cylindrical 3-DOF Parallel Robot," *Robotics and Autonomous System*, Vol. 42, pp. 31~46.

Wolf, A., Ottaviano, E., Shoham, M. and Ceccarelli, M., 2003, "Application of Line Geometry and Linear Complex Approximation to Singularity Analysis of the 3-DOF CaPaMan Parallel Manipulator," *Mechanism and Machine Theory*, Vol. 39, pp. 75~95.